Journal of Alloys and Compounds 765 (2018) 764–770

Contents lists available at ScienceDirect

Journal of Alloys and Compounds

journal homepage: http://www.elsevier.com/locate/jalcom

Highly tunable magnetoelectric response in dimensional gradient laminate composites of Fe-Ga alloy and $Pb(Mg_{1/3}Nb_{2/3})O_3$-$Pb(Zr,Ti)O_3$ single crystal

Haribabu Palneedi [a], Suok-Min Na [b], Geon-Tae Hwang [a], Mahesh Peddigari [a], Kwang Woo Shin [c], Kee Hoon Kim [c], Jungho Ryu [d, *]

[a] Functional Ceramics Group, Korea Institute of Materials Science, Changwon 51508, South Korea
[b] Department of Aerospace Engineering, University of Maryland, College Park, MD 20742, USA
[c] CeNSCMR, Department of Physics and Astronomy, Seoul National University, Seoul 08826, South Korea
[d] School of Materials Science and Engineering, Yeungnam University, Gyeongsan 38541, South Korea

A R T I C L E I N F O

Article history:
Received 14 March 2018
Received in revised form
8 May 2018
Accepted 9 May 2018
Available online 16 May 2018

Keywords:
Fe-Ga
PMN-PZT
Magnetoelectric
Composite
Tunable

A B S T R A C T

In this study, it is proposed and demonstrated that highly tunable magnetoelectric (ME) response can be achieved from magnetostrictive/piezoelectric laminate composites by integrating the effects of size variation and piezoelectric anisotropy. Tri-layered, rectangular ME composites with different aspect ratios were prepared using a magnetostrictive Fe-Ga alloy and a (011) oriented $Pb(Mg_{1/3}Nb_{2/3})O_3$-$Pb(Zr,Ti)O_3$ (PMN-PZT) piezoelectric single crystal. ME coefficients in the range of 0.25–2.2 V/cm·Oe and 2–75 V/cm·Oe in the off-resonance and resonance mode, respectively, were obtained from the composites. Magnetic sensitivity of the ME composites followed a similar trend in variation as that of their ME response with respect to the laminate size and applied magnetic field direction. The tunability of the ME response of the composites was correlated with the size dependent demagnetization and magnetic flux density distribution in the Fe-Ga alloy and direction dependent piezoelectric properties of the (011) PMN-PZT single crystal. In both the off-resonance and resonance modes, an order of magnitude large tunability could be attained in the ME coefficient of the composites. Such a highly tunable ME response will facilitate the development of ME based devices with controllable functionality.

1. Introduction

Multiferroic magnetoelectric (ME) materials have been intensively investigated due to their potential applications in magnetic sensors, energy harvesters, microwave devices, magnetic memories, and biomedical systems [1–5]. ME composites formed with piezoelectric and magnetostrictive components are more attractive for practical applications, due to their relatively strong ME coupling, compared to single phase ME compounds [6,7]. The strain-mediated ME coupling in composites, quantified in terms of the ME voltage coefficient, depends mainly on the efficiency of coupling between the magnetic and electric domains of the magnetostrictive and piezoelectric phases, respectively. Epoxy-bonded bulk laminate ME composites have been widely studied as they are comparatively simpler to be fabricated and easier to be adopted in the device design [8,9]. Besides the preservation of original physical characteristics of the individual phases, the absence of electrical leakage (from the magnetic constituent) and the greater mechanical coupling (through interfacial strain transfer) in the planar laminate composites would lead to their higher ME response than that could be obtained with other ME composite geometries.

Recently, Fe–Ga alloys have attracted great interest, for their use as a magnetostrictive component in ME composites [10–13]. Compared to the brittle and expensive magnetostrictive alloys Terfenol-D (Tb-Dy-Fe) and Metglas (Fe-B-Si), which are often employed in ME composites, Fe-Ga alloy is relatively inexpensive and exhibits a combination of high mechanical strength and good ductility, allowing it to be used in harsh and shock-prone environments (high temperature-high stress) [12,14,15]. Further, Fe-Ga alloys can be mass produced using cost-effective processes and easily prepared in different shapes [15–17]. Lead (Pb)-based

* Corresponding author.
E-mail address: jhryu@ynu.ac.kr (J. Ryu).

https://doi.org/10.1016/j.jallcom.2018.05.122
0925-8388/

piezoelectric single crystals such as PMN-PT [$Pb(Mg_{2/3}Nb_{1/3})O_3$-$PbTiO_3$] and PZN-PT [$Pb(Zn_{2/3}Nb_{1/3})O_3$-$PbTiO_3$], displaying high piezoelectric constants and electromechanical coupling coefficients, have been widely used in the fabrication of ME composites [18–21]. However, these single crystals show low phase transition temperature (~90 °C) and coercive electric field (~2.5 kV/cm). To extend the application range of these materials, PMN-PZT [$Pb(Mg_{2/3}$-$Nb_{1/3})O_3$-$Pb(Zr,Ti)O_3$] single crystals with improved phase transition temperature (~145 °C) and coercive electric field (~7 kV/cm) and optimized piezoelectric properties (by addition of a donor/acceptor) have been developed recently [22]. Based on the above considerations, we fabricated laminate ME composites using a magnetostrictive Fe-Ga alloy and a (011) oriented W-doped PMN-PZT single crystal, in this study.

Tailoring of the ME response in the bulk laminate composites has been done through different approaches such as (i) modification of the phase fraction of the constituent layers [23,24], (ii) employment of textured or single crystal ceramics with specially controlled and anisotropic piezoelectric properties [25,26], (iii) variation of dimensions and geometry of the constituent layers [27–29], and (iv) control of the properties of interfacial bonding layer and its thickness [30,31]. Although one can find several reports employing one of these individual approaches, no attempt had been made to combine any of them. In this study, we propose to integrate size variation and piezoelectric anisotropy strategies into the design of ME composites and investigate the effect of such a combination on their ME coupling. To exploit this idea, rectangular laminate ME composites were made using a Fe-Ga alloy with different aspect ratios (varied length but fixed width and thickness) and a (011) oriented PMN-PZT single crystal with anisotropic piezoelectric properties. Both off-resonant and resonant ME coefficients and magnetic sensitivity of the prepared composites were found to be strongly dependent on the length of the laminate, the anisotropy of the single crystal, and the applied magnetic field direction. An order of magnitude large tunability in ME response of the composites was observed, which could be correlated with demagnetization and magnetic flux density distribution in the Fe-Ga alloy and anisotropic piezoelectric properties of the PMN-PZT single crystal. This study demonstrates a feasible approach for realizing a large and highly tunable ME response from magnetostrictive/piezoelectric laminate composites.

2. Experimental methods

Tri-layered ME composites of Fe-Ga/PMN-PZT/Fe-Ga were prepared by epoxy bonding (3 M Scotch-Weld adhesive, cured at 80 °C for 4 h) the plates of polycrystalline a Fe-Ga alloy and a (011) oriented W-doped PMN-PZT single crystal (DPSC150-85, Ceracomp Co., Ltd., Korea) (Fig. 1(a)). The Fe-Ga alloy sheet was produced by induction melting technique followed by chill casting and subsequent hot rolling, as described elsewhere [16,17]. The Fe-Ga alloy had a composition of $(Fe_{0.81}Ga_{0.19})_{0.99}(NbC)_{0.1}$, where 1 mol% niobium carbide (NbC) particles (<10 μm) were added to the alloy to improve its ductility and rollability by suppressing gran boundary fracture. The (011) PMN-PZT single crystal was fabricated by solid state single crystal growth method, where the sample was cut to make its plane vector parallel to [011] direction [22]. The anisotropic piezoelectric properties of the (011) oriented PMN-PZT single crystal are provided in Table 1. In the ME composites prepared, the lengths of the Fe-Ga alloy plate and PMN-PZT plates were varied (l_{FeGa} or $l_{PMN\text{-}PZT} = 5$, 10, 15 mm) while their widths ($w_{Fe\text{-}Ga}$ or $w_{PMN\text{-}PZT} = 5$ mm) and thicknesses ($t_{Fe\text{-}Ga} = 0.5$ mm and $t_{PMN\text{-}PZT} = 0.3$ mm) were kept constant (Fig. 1(b)). The X-ray diffraction (XRD, D/Max 2200, Rigaku Corporation, Japan) patterns obtained from the surfaces of the Fe-Ga alloy and (011) PMN-PZT single crystal are shown in Fig. 2.

Prior to measuring the ME coupling properties of the samples, they were poled under an electric field of 1 kV/mm for 20 min at room temperature. The ME output voltage induced by the composites were measured in both off-resonance ($f = 1$ kHz, $H_{ac} = 1$ Oe) and resonance ($f = 25$–400 kHz) conditions. A superimposed AC and DC magnetic field was applied along the length and width directions of the ME composite (Fig. 1(a)) and the output voltage signal from in its thickness direction (transverse ME) was recorded using a lock-in amplifier (SR850 for lower than 100 kHz and SR844 for higher than 100 kHz, Stanford Research Systems, Sunnyvale, USA). The value of ME voltage coefficient (α_E) was calculated by dividing the measured output voltage by the thickness of PMN-PZT plate and the applied AC magnetic field. AC magnetic field sensitivity of the ME composite samples was evaluated following the procedure described elsewhere [32]. The ME sensor output voltage (V_{ME}) was measured at the corresponding optimum DC bias and resonance frequency of each composite sample where it showed maximum α_E in the off-resonance and resonance ME mode, respectively. Magnetic flux density distribution in the Fe-Ga alloy plate was estimated by a finite element model using COMSOL Multiphysics (version 5.2). In this model, the Fe-Ga alloy plates with dimensions identical to those used in the experiments were considered. The Fe-Ga alloy was assumed to have a relative permeability of 100 when placed in air and subjected to a H_{ac} of 1 Oe along its in-plane direction [33]. A magnetostatic insulating boundary condition was applied around the Fe-Ga alloy plate. The magnetic flux density distribution in response to the magnetic field applied was visualized along the center plane of the Fe-Ga alloy plate.

3. Results and discussion

The ME responses of the laminate composites obtained by the application of magnetic field along their length (*H//l*) and width (*H//w*) directions in the off-resonance and resonance modes are shown in Fig. 3. It is clear from these data that there are significant variations in the magnitudes of transverse ME coefficients α_{E31} (*H//w* or (*H*//[01 1])) and α_{E32} (*H//l* or *H*//[100]) depending on the length of the laminate, the anisotropy of the single crystal, and the direction of the applied magnetic field. Furthermore, in the off-resonance mode, the position of the maximum α_E peak was changed with respect to the above parameters (Fig. 3(a) and b). The peak position shifted towards lower magnetic bias with the increase in length of the laminate when *H//l* while a reverse trend in peak shift was observed when *H//w*. It can also be seen that the change in magnetic field direction resulted in reversal of the sign of ME curves. The values of maximum α_E obtained from the composites were in the range of 0.25–2.2 V/cm·Oe and 2–75 V/cm·Oe in the off-resonance and resonance modes, respectively (Fig. 3(c, f)). In both the modes, the relative change in ME response of the composites corresponds to an order of magnitude large tunability.

The magnitude of maximum α_E was higher when the magnetic field was applied in its length direction and the relative change was largest in the case of 15 mm-long sample (Fig. 3(c, f)). In both the directions of the applied magnetic field, the value of maximum α_E increased with the increase in length of the laminate. The high values of maximum α_E obtained from the Fe-Ga/(011) PMN-PZT/Fe-Ga composite, in both off-resonant (2.2 V/cm·Oe) and resonant (75 V/cm·Oe) modes, are found to be larger than those reported for Fe-Ga alloy based laminate ME composites (Table 2) [10–13]. Interestingly, the highest off-resonance ME coefficient obtained for the FeGa/PMNPZT composite (2.2 V/cm·Oe) was also observed to greater than that of the Ni/PMNPZT (1.05 V/cm·Oe) and FeBSi/PMNPZT (1.67 V/cm·Oe) composites, prepared with similar

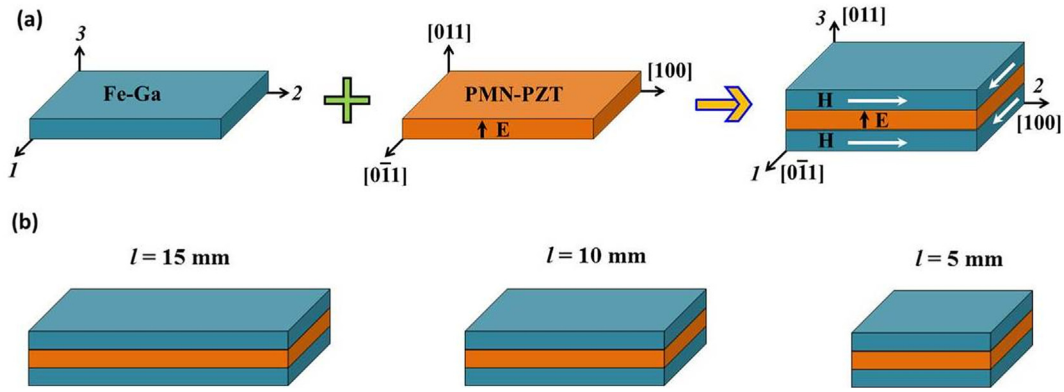

Fig. 1. Schematic drawings of the (a) laminate ME composite made with magnetostrictive Fe-Ga alloy and (011) PMN-PZT piezoelectric single crystal plates (b) Samples with different lengths but the same widths and thicknesses of the respective plates. Directions of the applied electrical poling field (E) for the PMN-PZT single crystal and magnetic field (H) for the ME measurement of the composite are also indicated.

Table 1
Piezoelectric properties of the (011) PMN-PZT single crystals (DPSC150-85, Ceracomp Co., Ltd., Korea) used in this study. Here d_{ij} is piezoelectric charge coefficient, S_{ij} elastic constant, k_{ij} electromechanical coupling factor, g_{ij} is piezoelectric voltage coefficient.

Material	d_{31} (pC/N)	d_{32} (pC/N)	S_{11} (pm^2/N)	S_{22} (pm^2/N)	k_{31}	k_{32}	g_{31} (10^{-3} mV/N)	g_{32} (10^{-3} mV/N)
(011) PMN-PZT	875	−2508	22	124	0.72	0.908	13	- 37.3

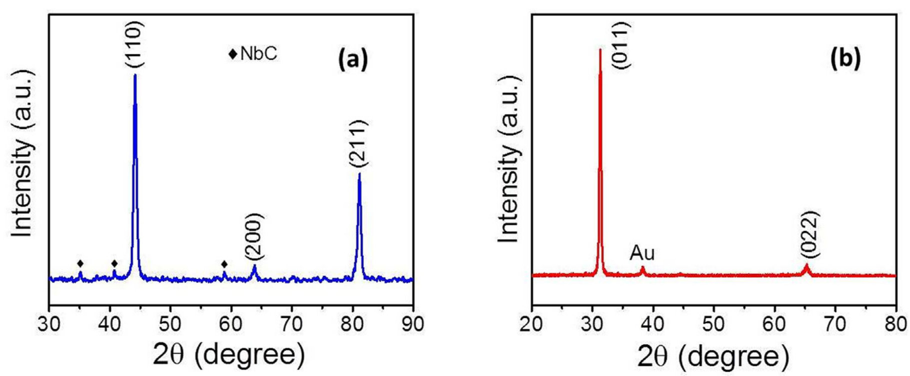

Fig. 2. XRD patterns of the (a) polycrystalline Fe-Ga alloy and (b) (011) oriented PMN-PZT single crystal.

dimensions and measured under same experimental conditions in a separate work. The observed variations in the magnitude and position of the maximum α_E and the sign of the ME response of the Fe-Ga/PMN-PZT composites can be related to the anisotropic piezoelectric properties of the PMN-PZT single crystal and the size dependent changes in demagnetization and magnetic flux density distribution of the magnetostrictive Fe-Ga alloy under the applied magnetic field.

The magnetic sensitivity data of the Fe-Ga/(011) PMN-PZT/Fe-Ga ME composites measured in terms of output voltage vs. AC magnetic field (H_{ac}) is plotted in Fig. 4. It can be observed that the induced ME voltage from the composite sensors exhibit a near linear proportionality to H_{ac} over a wide frequency range (μT to nT). The variation of magnetic sensitivity of the composite as a function of its length and with respect to the applied field direction followed similar trend as that of its ME coefficient, as expected. The 15 mm-long ME composite sample showed the highest magnetic sensitivity of up to 3 nT when *H//l* (*H*//[100]) and up to 25 nT when *H//w* (*H*//[01 1]) which are about one to two orders of magnitude higher than the sensitivity of 5 mm-long composite sample (100 nT when *H//l* and 200 nT when *H//w*). It is certain that the differences in ME response of the three composite samples have reflected in their magnetic sensitivities. The above observed results suggest that the magnetoelectric coefficient and magnetic sensitivity of the Fe-Ga/(011) PMN-PZT/Fe-Ga composites can be highly tuned by taking advantage of the piezoelectric anisotropy of the (011) PMN-PZT single crystal and the variation in dimensions of the laminate ME composite.

The transverse piezoelectric properties of the rhombohedral structured, relaxor ferroelectric single crystal materials, such as PMN-PT, PZN-PT, PMN−PZT are strongly dependent on the crystal cut directions [34,35]. These single crystals, when cut and poled along a non-polar direction, display greatly enhanced piezoelectric coefficients (d_{ij}, g_{ij}) and electromechanical coupling factors (k_{ij}). As shown in Fig. 5 (a), the rhombohedral single crystal has spontaneous polarization along the pseudo-cubic ⟨111⟩ directions, with eight possible dipole orientations. Poling along the polar [111] direction creates an unstable single-domain state, which leads to depoling as well as domain reorientation, resulting in significant hysteresis of strain versus electric field behavior and inferior piezoelectric properties of the single crystal. In contrast, the stable multi-domain configuration generated by poling along a non-polar

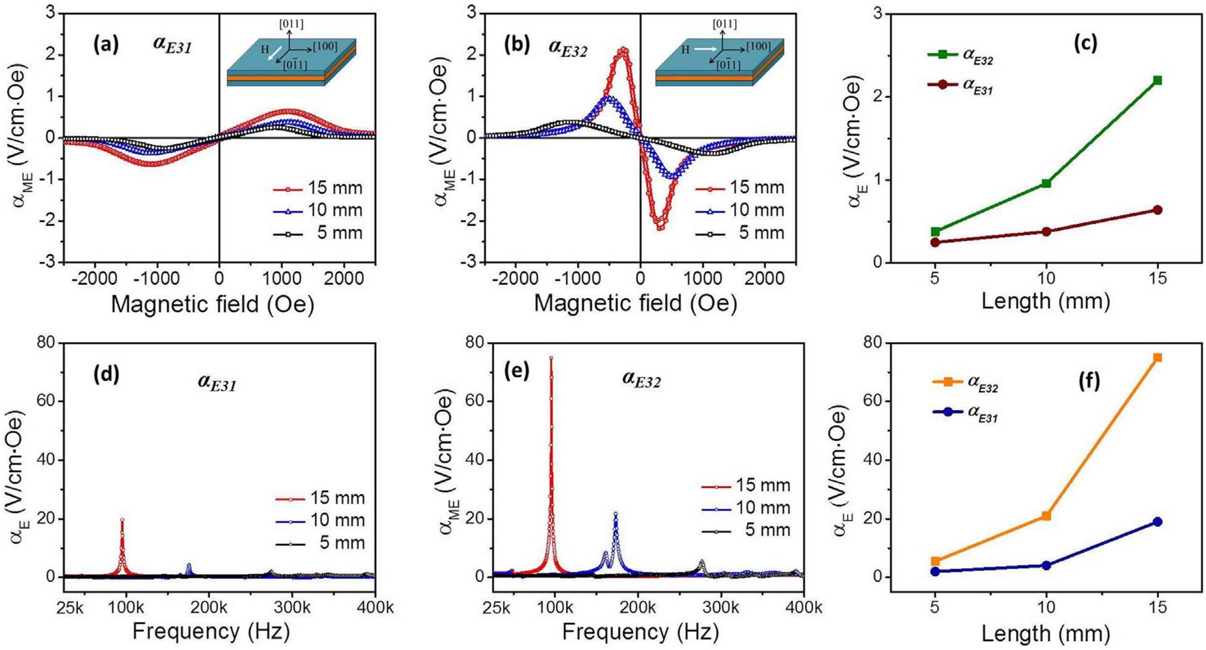

Fig. 3. Off-resonant (a, b) and resonant (d, e) ME coefficients of the Fe-Ga/(011)PMN-PZT/Fe-Ga laminates when magnetic field applied along their length (b, e) and width (a, d) directions. Variation of the maximum α_E values of the laminates as a function of their length in off-resonance and resonance ME modes are shown in (c) and (f), respectively.

Table 2
Comparison of the off-resonant and resonant ME coefficients obtained in this work with those reported for Fe-Ga based laminate ME composites.

ME composite	Sample geometry and dimensions	Off-resonant α_E (V/cm Oe)	resonant α_E (V/cm Oe)	Reference
$Fe_{80}Ga_{20}$/BT	circular, $12 \times 1.5\ mm^2$	0.0125	0.0285	[10]
(001) $Fe_{80}Ga_{20}$/PZT	rectangular, $14 \times 6 \times 0.5\ mm^3$	0.345	66	[11]
(001) $Fe_{80}Ga_{20}$/(001) PMN-PT	rectangular, $14 \times 6 \times 1\ mm^3$	1.01	70	[12]
$Fe_{81.4}Ga_{18.6}$/(011) PIN-PMN-PT	rectangular, $12 \times 4 \times 4\ mm^3$	1.38	–	[13]
$Fe_{81}Ga_{19}$/(011) PMN-PZT	rectangular, $15 \times 5 \times 0.5\ mm^3$	2.2	75	This work

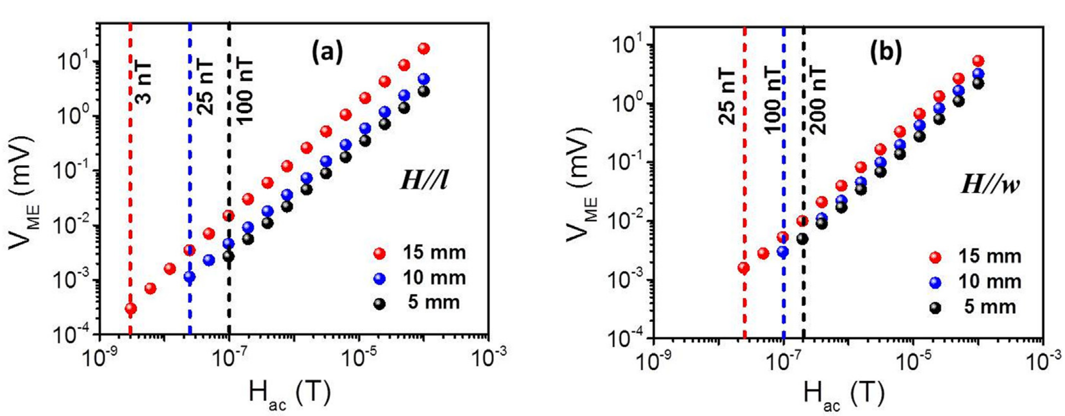

Fig. 4. Magnetic sensitivity of the ME composites under the application of the magnetic field along their (a) length and (b) width directions.

direction ([001] or [011]) gives rise to almost hysteresis-free strain behavior and enhanced piezoelectric properties of the single crystal. As noted in Table 1, the (011) oriented and poled PMN-PZT single crystal possesses large and anisotropic transverse piezoelectric properties. In d_{32} mode (working mode of the piezoelectric element, where 3 refers to the induced polarization direction and 2 refers to the applied stress direction), the d_{32}, g_{32}, and k_{32} values of the (011) oriented PMN-PZT single crystal are even much

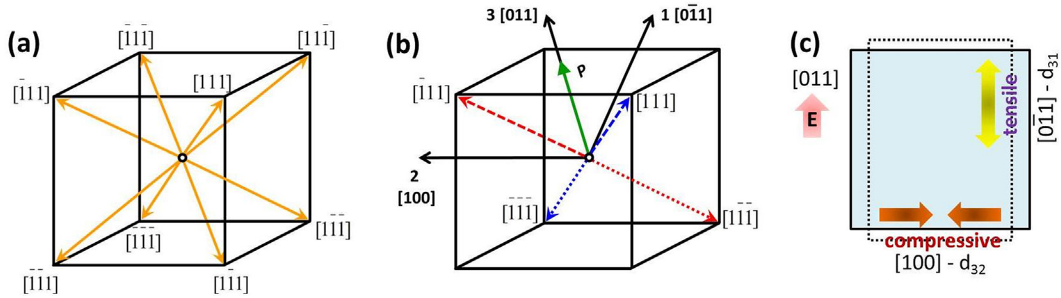

Fig. 5. Schematics of the (a) rhombohedral unit cell of PMN-PZT with eight possible ⟨111⟩ polarization directions. (b) and (c) domain configuration for the (011) oriented and poled PMN-PZT single crystal and corresponding changes of distortion in the d_{31} and d_{32} modes, respectively. Here, *P* denotes the direction of the electrical poling field applied to the single crystal.

higher than those of the (001) oriented PMN-PZT single crystal which possesses isotropic transverse piezoelectric properties [22].

Fig. 5 (b) shows the domain configuration of the PMN-PZT single crystal cut and poled along the [011] direction. Upon poling (E//[011]), each domain has one of the two possible dipole orientations [111] and [1 11] (dashed arrows), which switch to the [1 1 1] and [11 1] orientations (dotted arrows) by reversing the poling field (E//[011]). In the former case, the applied poling field will align the polarization vectors [111] and [1 11] to being closer to the [011] direction, which simultaneously induces a larger compressive strain along the [100] direction and a smaller tensile strain along the [01 1] direction as illustrated in Fig. 5 (c). This in turn leads to the different signs and magnitudes of the transverse piezoelectric properties of the single crystal (Table 1). As observed above in Fig. 3, the highly anisotropic α_E (with opposite signs of ME curves in off-resonance mode) exhibited by the Fe-Ga/(011) PMN-PZT/Fe-Ga composite in *H//l* (H//[100]) and *H//w* (H//[01 1]) configurations are due to the anisotropic transverse piezoelectric properties of the (011) PMN-PZT single crystal. The larger values of α_{E32} of the composites compared to their α_{E31} values can be attributed to the higher piezoelectric coefficients of the PMN-PZT single crystal in [100] direction (d_{32} mode) compared to those in the [01 1] direction (d_{31} mode).

The magnetic flux density of the magnetostrictive phase (B_m) is related to the ME voltage coefficient according to [36]:

$$\alpha_E = \frac{dE_i}{dH_a} = \frac{dE_i}{d\lambda} \times \frac{d\lambda}{dH_a} = \frac{dE_i}{d\lambda} \times \left(\frac{d\lambda}{dB_m} \times \frac{dB_m}{dH_a}\right) \quad (1)$$

where, E_i is the induced electric voltage in the piezoelectric phase, λ is the magnetostrictive strain, and H_a is the external magnetic field applied. The demagnetization in the magnetostrictive layer, which depends on its dimensions and geometry, can significantly influence the ME response of the composite. The demagnetization field (H_d) produced by the magnetic phase opposes the external magnetic field applied and thus the effective magnetic field (H_{eff}) in the sample is reduced. Consequently, the effective magnetic flux density (B_{eff}) in the magnetic phase will also be reduced as per the following relations [37]:

$$H_{eff} = H_a - H_d = H_a - MN_d \quad (2)$$

$$B_{eff} = \mu_0\left(H_{eff} + M\right) = \mu_0(H_a + M) - \mu_0 MN_d \quad (3)$$

where, M is magnetization, N_d is demagnetization factor ($0 \le N_d \le 1$), and μ_0 is magnetic permeability of free space. It is clear from the above relations that smaller demagnetization in the magnetic phase results in a larger effective magnetic induction and thus leads to a stronger ME coupling in the composite.

For a finite, rectangular ferromagnetic plate N_d can be approximated as $N_d \approx (wt/l^2)(\ln(4l/(w+t))-1)$, where *l, w, t* are its length, width, and thickness, respectively [23]. Fig. 6(a) shows the variation of N_d as a function of the length of the Fe-Ga alloy plate, where the quantity of N_d decreased with increase in its length. The FEM results of the simulated magnetic flux density distribution of the Fe-Ga alloy plate with different lengths, in the *H//l* and *H//w* conditions are shown in Fig. 6 (b). It was observed that the magnetic induction increases with increase in the length of Fe-Ga alloy plate in both directions, which can be related to the decrease in demagnetization with increase in the length. Therefore, the increase in magnitudes of α_{E31} and α_{E32} of the composite with increase in length can be due to the corresponding increase in *B* and decrease in N_d. The 5 mm-long Fe-Ga alloy plate exhibited a similar magnetic induction in

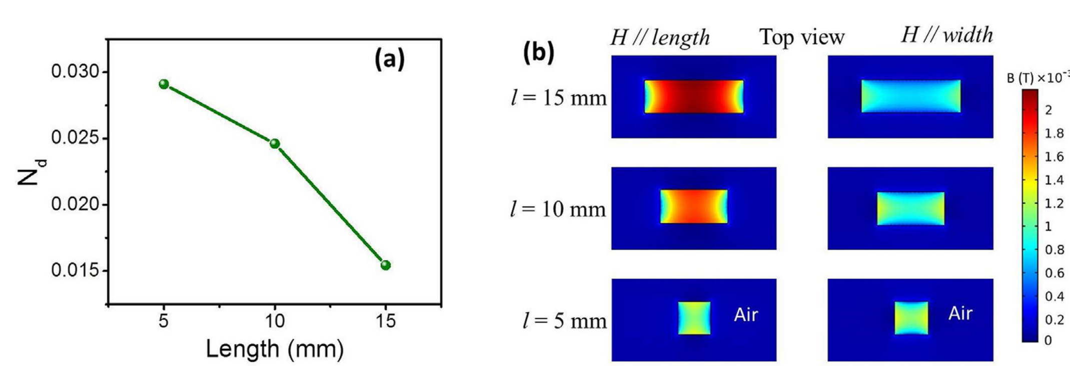

Fig. 6. (a) Variation of demagnetization factor of the Fe-Ga alloy plate as a function of its length. (b) FEM results of in-plane magnetic flux density distribution along the center plane of the Fe-Ga plate with different lengths when magnetic field is applied along its length and width directions.

both directions while the magnetic induction was stronger for *H//l* compared to that for *H*//*w* in the other two samples (15 mm- and 10 mm-long). Nevertheless, the magnitude of α_{E32} was larger than α_{E31} of the composite for all lengths, which explains the contribution of piezoelectric coefficients that are higher in the d_{32} mode (H//[100]) compared to that in the d_{32} mode (H//[01 1]) configuration.

4. Conclusions

In summary, we fabricated rectangular laminate ME composites of Fe-Ga/(011) PMN-PZT/Fe-Ga with different aspect ratios. The effect of the combination of piezoelectric anisotropy of the (011) oriented PMN-PZT single crystal and size variation of the Fe-Ga alloy on the ME response of the composite was investigated. An order of magnitude large tunability in ME coefficient of the composites, which is in the range of 0.25–2.2 V/cm·Oe and 2–75 V/cm·Oe in the off-resonance and resonance modes, respectively, was observed. The high ME coefficients of the Fe-Ga/(011) PMN-PZT/Fe-Ga composite, obtained in both off-resonant (2.2 V/cm·Oe) and resonant (75 V/cm·Oe) modes, are also larger than those reported for Fe-Ga based laminate ME composites. The differences in ME responses of the composites have reflected in their magnetic sensitivities, which were found to be in the range of 3–200 nT. The tunability of the ME coefficient of the composites, strongly dependent on the length of the laminate and the applied magnetic field direction, was correlated with demagnetization and magnetic flux density distribution in the Fe-Ga alloy as well as anisotropic piezoelectric properties of the (011) PMN-PZT single crystal. This study demonstrates that ME composites with highly tunable ME response can be developed by adopting a feasible combination of oriented piezoelectric single crystals with anisotropic properties and magnetostrictive alloys with appropriate dimensions.

Acknowledgements

This research work was supported by the Basic Science Research Program of the National Research Foundation (NRF) of Korea funded by the Ministry of Science, ICT & Future Planning (NRF-2016R1A2B4011663) and internal R&D program of KIMS (Grant No. PNK5810) and Yeungnam University (Grant No. 218A580001). The work of K.H.K. at Seoul National University was financially supported by the National Creative Research Initiative (Grant No. 2010-0018300) through the NRF of Korea.

References

[1] J. Ma, J. Hu, Z. Li, C.-W. Nan, Recent progress in multiferroic magnetoelectric composites: from bulk to thin films, Adv. Mater. 23 (2011) 1062–1087.
[2] Y. Zhou, J.-W. Kim, S. Dong, S. Priya, J. Wang, J. Ryu, Applications of multiferroic magnetoelectric composites, in: J. Wang (Ed.), Multiferroic Materials: Properties, Techniques, and Applications, CRC Press, Boca Raton, FL, 2017, pp. 215–254.
[3] V. Annapureddy, H. Palneedi, G.-T. Hwang, M. Peddigari, D.-Y. Jeong, W.-H. Yoon, K.-H. Kim, J. Ryu, Magnetic energy harvesting with magnetoelectrics: an emerging technology for self-powered autonomous systems, RSC Sustain. Energy Fuels 1 (2017) 2039–2052.
[4] M.M. Vopson, Fundamentals of multiferroic materials and their possible applications, Crit. Rev. Solid State Mater. Sci. 40 (2015) 223–250.
[5] M.I. Bichurin, D. Viehland, G. Srinivasan, Magnetoelectric interactions in ferromagnetic-piezoelectric layered structures: phenomena and devices, J. Electroceram. 19 (2007) 243–250.
[6] J. Ryu, S. Priya, K. Uchino, H.-E. Kim, Magnetoelectric effect in composites of magnetostrictive and piezoelectric materials, J. Electroceram. 8 (2002) 107–119.
[7] J. Ryu, C.-W. Baek, Y.-S. Lee, N.-K. Oh, G. Han, J.-W. Kim, B.-D. Hahn, J.-J. Choi, W.-H. Yoon, J.-H. Choi, D.-S. Park, D.-Y. Jeong, Enhancement of multiferroic properties in $BiFeO_3$–$Ba(Cu_{1/3}Nb_{2/3})O_3$: film fabricated by aerosol deposition, J. Am. Ceram. Soc. 94 (2011) 355–358.
[8] J. Zhai, Z. Xing, S. Dong, J. Li, D. Viehland, Magnetoelectric laminate composites: an overview, J. Am. Ceram. Soc. 91 (2008) 351–358.
[9] J. Ryu, A.V. Carazo, K. Uchino, H.-E. Kim, Magnetoelectric properties in piezoelectric and magnetostrictive laminate composites, Jpn. J. Appl. Phys. 40 (2001) 4948.
[10] L. Wang, Z. Du, C. Fan, L. Xu, H. Zhang, D. Zhao, Magnetoelectric properties of Fe–Ga/BaTiO3 laminate composites, J. Alloys Compd. 509 (2011) 508–511.
[11] S. Dong, J. Zhai, F. Bai, J. Li, D. Viehland, T.A. Lograsso, Magnetostrictive and magnetoelectric behavior of Fe–20at.% Ga/Pb(Zr,Ti)O_3 laminates, J. Appl. Phys. 97 (2005), 103902.
[12] S. Dong, J. Zhai, N. Wang, F. Bai, J. Li, D. Viehland, T.A. Lograsso, Fe–Ga/$Pb(Mg_{1/3}Nb_{2/3})O_3$–$PbTiO_3$ magnetoelectric laminate composites, Appl. Phys. Lett. 87 (2005), 222504.
[13] P. Finkel, R. Pérez Moyet, M. Wun-Fogle, J. Restorff, J. Kosior, M. Staruch, J. Stace, A. Amin, Non-resonant magnetoelectric energy harvesting utilizing phase transformation in relaxor ferroelectric single crystals, Actuators 5 (2016) 2.
[14] R. Myers, R.A. Islam, M. Karmarkar, S. Priya, Magnetoelectric laminate composite based tachometer for harsh environment applications, Appl. Phys. Lett. 91 (2007) 122904.
[15] A. Jayasimha, A.B. Flatau, A review of magnetostrictive iron–gallium alloys, Smart Mater. Struct. 20 (2011), 043001.
[16] S.-M. Na, A. Passel, P. Downey, A. Flatau, Magnetostrictive Fe–Ga alloy strips with a preferred orientation for lamination actuators, Phys. Status Solidi. A 210 (2013) 1076–1082.
[17] V. Annapureddy, S.-M. Na, G.-T. Hwang, M.G. Kang, R. Sriramdas, H. Palneedi, W.-H. Yoon, B.-D. Hahn, J.-W. Kim, C.-W. Ahn, D.-S. Park, J.-J. Choi, D.-Y. Jeong, A.B. Flatau, M. Peddigari, S. Priya, K.-H. Kim, J. Ryu, Exceeding milli-watt powering magneto-mechano-electric generator for standalone-powered electronics, Energy Environ. Sci. (2018), https://doi.org/10.1039/c7ee03429f.
[18] T. Wu, A. Bur, K. Wong, J.L. Hockel, C.-J. Hsu, H.K.D. Kim, K.L. Wang, G.P. Carman, Electric-poling-induced magnetic anisotropy and electric-field-induced magnetization reorientation in magnetoelectric Ni/(011) [$Pb(Mg_{1/3}Nb_{2/3})O_3$](1-x)-[$PbTiO_3$]x heterostructure, J. Appl. Phys. 109 (2011), 07D732.
[19] Z. Wang, Y. Zhang, R. Viswan, Y. Li, H. Luo, J. Li, D. Viehland, Electrical and thermal control of magnetic coercive field in ferromagnetic/ferroelectric heterostructures, Phys. Rev. B 89 (2014), 035118.
[20] J. Lou, M. Liu, D. Reed, Y. Ren, N.X. Sun, Giant electric field tuning of magnetism in novel multiferroic FeGaB/lead zinc niobate–lead titanate (PZN-PT) heterostructures, Adv. Mater. 21 (2009) 4711–4715.
[21] S. Dong, J. Zhai, Z. Xing, J. Li, D. Viehland, Giant magnetoelectric effect (under a dc magnetic bias of 2Oe) in laminate composites of FeBSiC alloy ribbons and $Pb(Zn_{1/3},Nb_{2/3})O_3$–7%$PbTiO_3$ fibers, Appl. Phys. Lett. 91 (2007), 022915.
[22] H.-T. Oh, J.-Y. Lee, H.-Y. Lee, Mn-modified PMN-PZT [$Pb(Mg_{1/3}Nb_{2/3})O_3$-Pb(Zr,Ti)O_3] single crystals for high power piezoelectric transducers, J. Kor. Ceram. Soc. 54 (2017) 150–157.
[23] Y. Zhou, S.C. Yang, D.J. Apo, D. Maurya, S. Priya, Tunable self-biased magnetoelectric response in homogenous laminates, Appl. Phys. Lett. 101 (2012), 232905.
[24] D. Rajaram Patil, R.C. Kambale, Y. Chai, W.-H. Yoon, D.-Y. Jeong, D.-S. Park, J.-W. Kim, J.-J. Choi, C.-W. Ahn, B.-D. Hahn, S. Zhang, K. Hoon Kim, J. Ryu, Multiple broadband magnetoelectric response in thickness-controlled Ni/[011] $Pb(Mg_{1/3}Nb_{2/3})O_3$-Pb(Zr,Ti)$_{O3}$ single crystal/Ni laminates, Appl. Phys. Lett. 103 (2013), 052907.
[25] J.V. Vidal, A.A. Timopheev, A.L. Kholkin, N.A. Sobolev, Anisotropy of the magnetoelectric effect in tri-layered composites based on single-crystalline piezoelectrics, Vacuum 122 (2015) 286–292.
[26] D. Rajaram Patil, Y. Chai, R.C. Kambale, B.-G. Jeon, K. Yoo, J. Ryu, W.-H. Yoon, D.-S. Park, D.-Y. Jeong, S.-G. Lee, J. Lee, J.-H. Nam, J.-H. Cho, B.-I. Kim, K. Hoon Kim, Enhancement of resonant and non-resonant magnetoelectric coupling in multiferroic laminates with anisotropic piezoelectric properties, Appl. Phys. Lett. 102 (2013), 062909.
[27] D.A. Pan, J.J. Tian, S.G. Zhang, J.S. Sun, A.A. Volinsky, L.J. Qiao, Geometry effects on magnetoelectric performance of layered Ni/PZT composites, Mater. Sci. Eng. B 163 (2009) 114–119.
[28] M.P. Silva, P. Martins, A. Lasheras, J. Gutiérrez, J.M. Barandiarán, S. Lanceros-Mendez, Size effects on the magnetoelectric response on PVDF/Vitrovac 4040 laminate composites, J. Magn. Magn. Mater. 377 (2015) 29–33.
[29] Z. Chu, H. Shi, W. Shi, G. Liu, J. Wu, J. Yang, S. Dong, Enhanced resonance magnetoelectric coupling in (1-1) connectivity composites, Adv. Mater. 29 (2017) 1606022.
[30] M. Li, D. Hasanyan, Y. Wang, J. Gao, J. Li, D. Viehland, Theoretical modelling of magnetoelectric effects in multi-push–pull mode Metglas/piezo-fibre laminates, J. Phys. D Appl. Phys. 45 (2012), 355002.
[31] M. Silva, S. Reis, C.S. Lehmann, P. Martins, S. Lanceros-Mendez, A. Lasheras, J. Gutiérrez, J.M. Barandiarán, Optimization of the magnetoelectric response of poly(vinylidene fluoride)/epoxy/vitrovac laminates, ACS Appl. Mater. Interfaces 5 (2013) 10912–10919.
[32] V. Annapureddy, H. Palneedi, W.-H. Yoon, D.-S. Park, J.-J. Choi, B.-D. Hahn, C.-W. Ahn, J.-W. Kim, D.-Y. Jeong, J. Ryu, A pT/$\sqrt{Hz}$ sensitivity ac magnetic field sensor based on magnetoelectric composites using low-loss piezoelectric single crystals, Sens. Actuators A Phys. 260 (2017) 206–211.
[33] T. Ueno, E. Summers, M. Wun-Fogle, T. Higuchi, Micro-magnetostrictive vibrator using iron–gallium alloy, Sens. Actuators A Phys. 148 (2008) 280–284.
[34] S.-E. Park, T.R. Shrout, Ultrahigh strain and piezoelectric behavior in relaxor based ferroelectric single crystals, J. Appl. Phys. 82 (1997) 1804–1811.

[35] S. Wada, H. Kakemoto, T. Tsurumi, Enhanced piezoelectric properties of piezoelectric single crystals by domain engineering, Mater. Trans. 45 (2004) 178–187.
[36] Z. Fang, S.G. Lu, F. Li, S. Datta, Q.M. Zhang, M.E. Tahchi, Enhancing the magnetoelectric response of Metglas/polyvinylidene fluoride laminates by exploiting the flux concentration effect, Appl. Phys. Lett. 95 (2009) 112903.
[37] X. Cui, S. Dong, Theoretical analyses on effective magnetoelectric coupling coefficients in piezoelectric/piezomagnetic laminates, J. Appl. Phys. 109 (2011), 083903.